Co-Existence of Ductile, Semi-Ductile, and Brittle Fractures of Polycarbonate

FENG-CHIH CHANG* and LINE-HWA CHU†

Institute of Applied Chemistry, National Chiao-Tung University, Hsinchu, Taiwan, Republic of China

SYNOPSIS

The ductile–brittle transition behavior of polycarbonate and methylmethacrylate–butadiene–styrene (MBS) elastomer modified polycarbonate has been investigated in terms of notch radius and temperature. At −40°C and 21-mil notch radius, polycarbonate fractures in three possible modes, ductile (25%), semi-ductile (50%), and brittle (25%). This semi-ductile mode fracture has never been reported previously with brittle characterization, but to a greater extent in localized shear yielding on the fracture surface and intermediate toughness. A two-dimensional fracture mode diagram in terms of temperature and notch radius has been constructed to interpret the observed phenomena. This diagram can also predict the existence of other conditions under which the triplet fracture modes may also occur. Another unstable zone has also been identified where the fracture occurs in either ductile mode or brittle mode over a broad temperature range, instead of the narrow temperature range typically observed for polycarbonate. A model based on the excessive precrack strain just below yielding due to the greater notch radius is proposed to explain such observed semi-ductile mode fracture.

INTRODUCTION

Polycarbonate (PC) is an engineering thermoplastic with outstanding properties including transparency, high T_g, toughness, and good dimensional stability. Polycarbonate exhibits a distinctive ductile–brittle transition in response to a number of variables including temperature, rate, thickness, orientation, annealing, notch radius, molecular weight, elastomer content, and molding condition. The mechanism of this sharp transition is not fully understood due to its extreme complexity, and the subject has attracted great attention. A competition between shear yielding and crazing has been frequently proposed to account for the phenomenon.[1] Brown proposed a mixed-mode crack propagation based on specimen thickness to predict the existence of a brittle–ductile transition.[2] Hull et al. described the ductile fracture as large-scale plastic deformation in the notch root where fracture occurs by tearing processes and the

stress is maintained on the section at a much higher level than in a brittle fracture.[3] We propose the existence of a critical precrack plastic zone in determining the ductile–brittle transition.[4,5] For polycarbonate, the ductile–brittle transition as a function of temperature has been extensively investigated.[3,4,6–12] The temperature at the ductile–brittle transition (DBTT) may not be a single temperature, but rather a transition range, and the range varies from one material to another. In a standard notched (10 mil) polycarbonate specimen, a transition range within 2°C is obtainable experimentally. However, most literature does not describe such a narrow temperature range. Identical polycarbonate specimens exhibiting both ductile and brittle failures at one temperature can be obtained fairly easily.[4] Stress concentration in the specimen takes place at the notch and the notch tip constitutes a constraint to plastic formation. Therefore the effect of notch radius on PC fracture has also attracted intensive studies.[7,10,13–16] Polycarbonate fractures are normally either ductile (characteristic with extensive yielding and lateral contraction) or brittle (relatively smooth surface without lateral contraction). Two types of semi-ductile fractures have also been reported.[16,17] Fraser et al. studied four-point bend Charpy impact

---

tests on high MW $\frac{1}{8}$-inch thickness PC and discovered a semi-ductile type fracture with intermediate toughness by using notch radius between 7 and 10 mil.[16] The fracture surface of this semi-ductile specimen shows the front section to exhibit a typically ductile mode with extensive plastic flow and clear lateral contraction, while the back section shows a typical brittle mode. A very similar observation was also made by Dekkers et al. in the rubber modified blends of PPO/Nylon 6,6 and PC/PBT at intermediate strain rate and blunt notched specimens.[18] They named such an intermediate toughness fracture as a ductile tearing instability and interpreted it in terms of tearing modulus. They also reported that similar results were not found on polycarbonate over a wide range of test speeds and temperature. Another type of semi-ductile fracture of PC with intermediate thickness (0.173 inch) was reported by Yee, where the fracture surface is distinguished by a triangular flat and mirro-like area just behind the notch.[17] We also observed a similar result on $\frac{1}{4}$-inch thick specimens at high temperature and slow deformation rate.[19] Here we wish to report yet another type of semi-ductile fracture which has not been reported previously. In addition, we made the unusual discovery that the three modes of fractures—ductile, semi-ductile, and brittle—can actually co-exist under the same conditions.

EXPERIMENTAL

Notching of $\frac{1}{8}$-inch specimens was carried out using a single tooth cutter at ambient conditions with a radius of 2.5, 5, 10, and 20 mil. The actual notched radii were measured and calculated from a few selected freshly notched specimens using photomicrographs and turned out to be 3.3, 5.7, 10.6, and 21 mil, respectively. The rest of the experimental procedures were described previously.[4,5] Polycarbonate with a melt flow rate of 15 has been exclusively employed in this study.

RESULTS AND DISCUSSION

The effects of varying notch radius on polymer fracture behavior include stress concentration and rate dependency. These two are actually interrelated to some degree, and will be discussed separately below.

Theoretical Background of Notch Sensitivity

The theoretical cohesive strength of most materials is about $E/15$ where E is the Young modulus.

Scratches, cracks, and other imperfections concentrate stress; therefore, a real material has much lower strength. This is why in impact testing we need to study the effects of notches of varying dimensions. The detrimental effect of a scratch, crack, or an artificial notch is, on the basis of work of Inglis[20] and Griffith,[21] characterized by

$$\rho_t = 1 + 2(a/\rho)^{1/2}$$

where ρ_t is the stress at the end of the major axis, $2a$ is the length of the major axis and ρ is the radius of curvature at the bottom of the notch. Qualitatively the above equation is sufficient to note the detrimental effects produced by a crack; the sharper the crack tip, the greater the resulting K_t. Since the stress at the crack tip is singular, then clearly the yield criterion is exceeded in some zone in the crack tip region. The plastic deformation that occurs around the crack effectively blunts the crack tip; the degree of crack tip blunting that is incurred largely controls the measured toughness and the mode of crack growth. An estimation of this effect may be made by considering the elastic stress, σ_{11}, at a small distance, r, ahead of the tip of an elliptical crack of the major axis $2a$, in an infinite sheet and the solution for stresses around the elliptical hole is,

$$\sigma_{11} = \sigma_0 \left(\frac{a}{2r}\right)^{1/2} \frac{(1 + \rho/r)}{(1 + \rho/2r)^{3/2}}$$

Kinloch[22] and Yamini[23] proposed that fracture takes place when a critical stress is attained which acts over a certain distance, c, ahead of the crack tip; then $\sigma_{11} = \sigma_{tc}$ and the above equation becomes

$$\sigma_{tc} = \sigma_c \left(\frac{a}{2c}\right)^{1/2} \frac{(1 + \rho_c/c)}{(1 + \rho_c/2c)^{3/2}}$$

where ρ_c is the crack tip radius and σ_c is the applied stress at fracture. We can obtain the equation relating notch radius and stress-intensity factor as

$$\frac{K_{Ic}}{K_{Ics}} = \frac{(1 + \rho_c/2c)^{3/2}}{(1 + \rho_c/c)}$$

where $K_{Ics} = \sigma_{tc}\sqrt{2\pi c}$ may be interpreted as the intensity factor at the distance c ahead of the crack tip. Except for $\rho_c/c < 3$, K_{Ic}/K_{Ics} shows a slight drop, the higher value of notch radius ρ_c results in rapid increase of K_{Ic}. Although the application of above model has its foundations in LEFM, it can only cope with those situations of relatively moderate plasticity. However, this model does demonstrate that
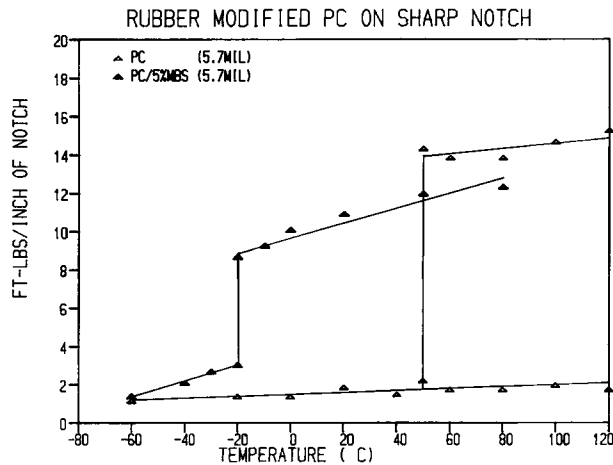
Figure 1 Impact strengths of PC and PC/5%MBS at 5.7 mil notch radius.

greater fracture stress is required for a greater notch radius. Coupled with our previously proposed model,[5] the greater stress required for crack initiation will result in a larger precrack plastic zone and eventually exceeds a critical value for brittle–ductile transition. Therefore the most important factor of notch radius which affects fracture behavior is the delay in the onset of crack initiation which allows the continuous growth of a precrack plastic zone and eventually exceeds a critical value for brittle–ductile transition.

Effect of Notch Radius on Strain Rate

The typical Izod impact test has a hammer striking velocity of about 3 m/s. In the notched beam tests, the strain rate at the notch tip is considerably higher and has been estimated[24] to be of the order of 5 $\times 10^3$ s^{-1}. The yield behavior of glassy polymers is dependent upon temperature and rate. Bauwens-Crowet[25] studied the dependence of polycarbonate yield stress on strain rate under different temperatures and modelled this dependence using the Eyring theory of viscosity.[26,27]

$$\frac{|\sigma_y|}{T} = \frac{\Delta E^*}{v^*T} + \left(\frac{R}{v^*}\right)\ln(\dot{e}/A_E)$$

where R is the gas constant, v^* is the activation volume and A_E is a constant. It is easily understood from the above equation that higher strain rate resulting from a sharper notch will cause an increase in yield stress. That means that under the same hammer impact rate conditions, the smaller notch radius will result in higher yield stress, while the

breaking stress (crazing stress) is normally quite rate and temperature independent. Such a time-dependent mechanical property in glassy polymers has been well recognized. Higher yield stress will produce a relatively smaller precrack plastic zone at the onset of crack initiation and the sample therefore tends to be more brittle. The addition of elastomer which results in lower yield stress can, at least partially, account for reducing the matrix notch sensitivity.

Effect of Elastomer

We made extensive studies on the effects of MBS elastomer on the ductile–brittle transition of polycarbonates using the standard 10-mil notch radius.[4] Reduced notch sensitivity is one of the major reasons why elastomers toughen brittle matrices. The presence of elastomer above its T_g is able to relieve the yield stress increase caused by the plane strain condition and enhances the shear yielding mechanism. Our previously proposed critical precrack plastic zone model offers a simple explanation of the rubber toughening mechanism.[4,5] The presence of elastomer in a matrix reduces yield stress and effectively resists crack initiation. This allows the precrack plastic zone to grow above a critical value and a crack developed later will result in ductile tearing. Figure 1 shows the impact strength of the 5.7-mil notched polycarbonate with and without 5% elastomer. The unmodified PC exhibits brittle fractures up to around 50°C. Above 50°C, PC exhibits unstable fractures, fracturing in either the ductile or brittle mode. This uncharacteristic PC behavior is quite unusual in comparison with the standard 10-mil notched specimens with clear ductile–brittle tran-
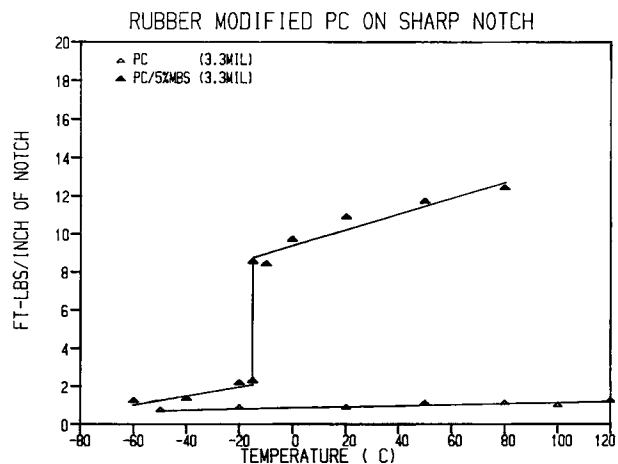

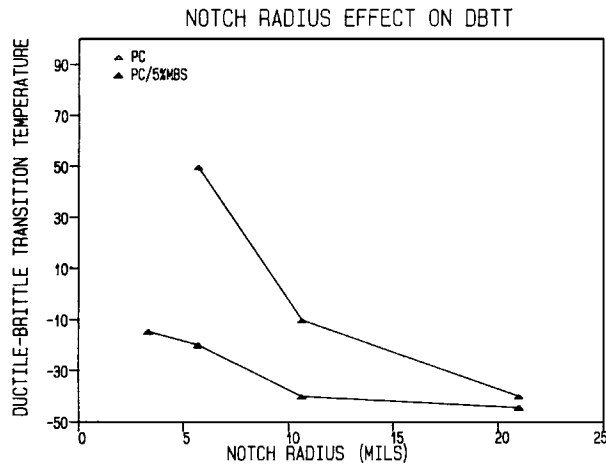**Figure 2** Impact strengths of PC and PC/5%MBS at 3.3 mil notch radius.

Figure 3 Effect of notch radius on PC and PC/5%MBS ductile–brittle transition temperature.

Figure 5 Photographs of 21 mil notch radius PC fracture surfaces at −40°C, (A) ductile mode, impact strength = 12.2 ft-lb/in; (B) semi-ductile mode, impact strength = 8.2 ft-lb/in; (C) brittle mode, impact strength = 2.2 ft-lb/in.

sition temperatures. That means the 10-mil notched PC specimens fracture essentially all in ductile mode above the DBTT and all in brittle mode below the DBTT. The elastomer modified PC has the DBTT at −20°C and the fracture is either ductile or brittle at that temperature. Specimens with even smaller notch radii (3.3 mil) fracture in the brittle mode up to PCS T_g with nearly constant low impact strength (Fig. 2). The 5% MBS modified PC shows the clean DBTT at −15°C. The brittle failure impact strength of the elastomer modified PC is considerably higher than the unmodified PC and this can be interpreted as being due to a dual fracture mode mechanism previously proposed.[4] Figure 3 summarizes the re-
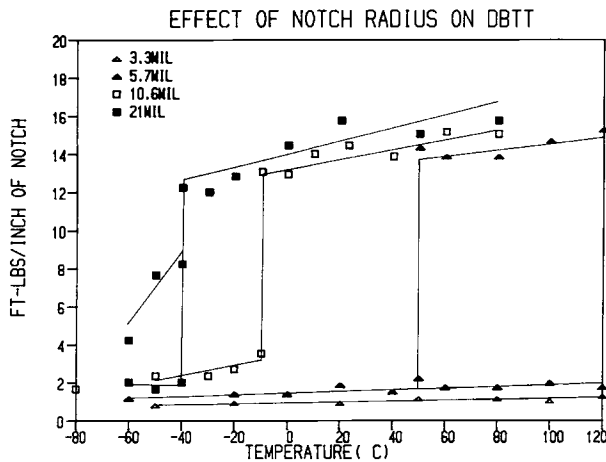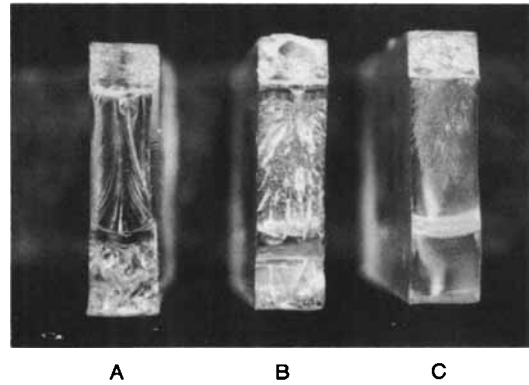
lation between notch radius and the DBTT of PC. The difference in DBTT is higher at low notch radius but gradually decreases and approaches zero as the notch radius is increased to above 20 mil (Fig. 3). These results are consistent with the commonly accepted concept that the presence of elastomer reduces notch impact sensitivity.

Effect of Notch Radius on DBTT

The impact strengths of polycarbonates of varying notch radii and temperatures are shown in Figure 4. The results from notch radius of 10 mil or less have been discussed previously and we will concentrate on the results from the notch radius of 21 mil. For ductile fractures, the greater notch radius has slightly higher impact strength as would be expected. At −40°C, three potential modes of fractures coexist with impact strengths of about 12, 8, and 2 ft lb/in respectively. The photographs of these three types fracture surfaces are shown in Figure 5. The appearance of the ductile fracture surface [Fig. 5(A)] is similar to any other ductile fracture surface and characterized by lateral contraction and extensive yielding. The brittle fracture surface [Fig. 5(C)] is again like any other brittle fracture specimen, showing various flat and rough patterns and no signs of lateral contraction.

The intermediate toughness surface [Fig. 5(B)] shows much more roughness covering the whole specimen with no signs of lateral contraction. In order to compare the surface morphologies more closely, scanning electron microscopy (SEM) with magnifications of ×20, ×100, and ×2000 were taken at different locations on the surfaces (Figs. 6–8).

Figure 4 Effect of notch radius on PC impact strength at varying test temperatures.

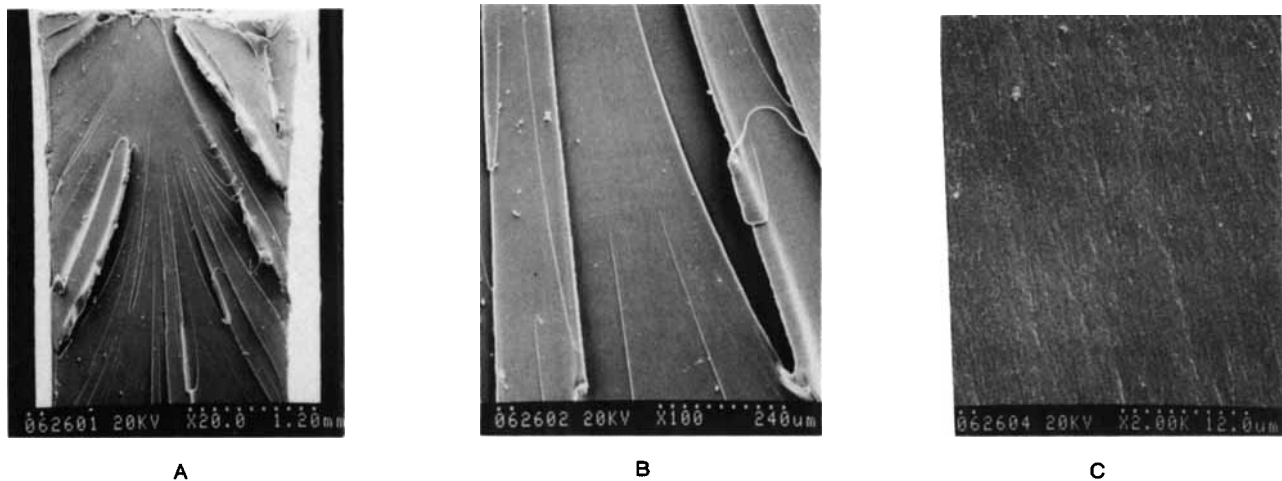**Figure 6** SEM micrographs of the ductile fracture surface, (A) original magnification ×20, front portion; (B) original magnification ×100, middle section; (C) original magnification ×2000, middle section.

Figure 6 shows the selected SEM micrographs of polycarbonate ductile fracture surfaces where extensive plastic flow and lateral contraction on both sides can be easily observed. Figure 7(A) is the surface of this semi-ductile fracture specimen in ×20 magnification showing a very rough surface but without suck-in from both sides. The higher magnifications of this specimen [Fig. 7(B,D)] clearly show extensive but localized tearing-type shear yielding.

Figure 7(C) shows the interesting morphology of the elliptical plane strain zone near the center of the notch root which consists of several elliptical zones and a pair of half moon marks on both sides between ellipses 2 and 3. Figure 8 shows the SEM micrographs of the brittle fracture specimen which are similar to the surface of the semi-ductile specimen except that the degree of roughness is much lower. Direct comparison between Figures 7(B) and 8(B) clearly demonstrates that the degree of localized shear yielding is significantly higher in the semi-ductile one [Fig. 7(B)]. The brittle fracture surface [Fig. 8(B)] shows very little tearing type yielding in comparison with the semi-ductile one. This brittle fracture surface shows such roughness only on the front portion of the surface (close to the notch) and a mirror-like flat surface on the rear end of the specimen [Fig. 5(C)], while the semi-ductile one has about the same roughness throughout the whole surface [Fig. 5(B)]. Combining the area and degree of roughness, the resultant semi-ductile toughness is about 2 to 4 times greater than the brittle one. When the testing temperatures are decreased to below 40°C (Fig. 4), only two modes of fracture co-

exist. The impact strength of the semi-ductile fracture decreases with the decrease of temperature and eventually approaches the level of brittle fracture at around −80°C.

In order to further understand the probability of each individual mode in the temperature range from −30°C to −60°C, a total of 50 specimens were prepared at the same time and the results are listed in Table I. At −30°C, all 5 specimens (or 100%) fractured in the ductile mode. At the critical temperature −40°C, about 25% fractured in the ductile, 50% in the semi-ductile, and 25% in the brittle mode. When the testing temperature was reduced to −50°C, 70% of the specimens fractured in the semi-ductile, 30% in the brittle, and none in the ductile mode. As the temperature was further reduced to −60°C, half fractured in the semi-ductile mode with a significant decrease in impact strength and the other half fractured in the brittle mode. Comparing the surface morphologies from these three types of failures, the semi-ductile type shows more characteristic features of brittle fracture than of ductile fracture. Lateral contraction is the common characteristic of ductile tearing in most pseuductile materials. The semi-ductile fracture basically is brittle failure with much more localized shear yielding. According to our previous proposed model[5] this mode of failure is due to the propagating crack front proceeding along with the front line of the extending plastic zone. This semi-ductile mode can also be interpreted as the crack propagating into a region possessing greater strain due to the greater notch radius delaying the onset of crack initiation. Since the strain ahead of crack tip is already raised almost to its shear yielding
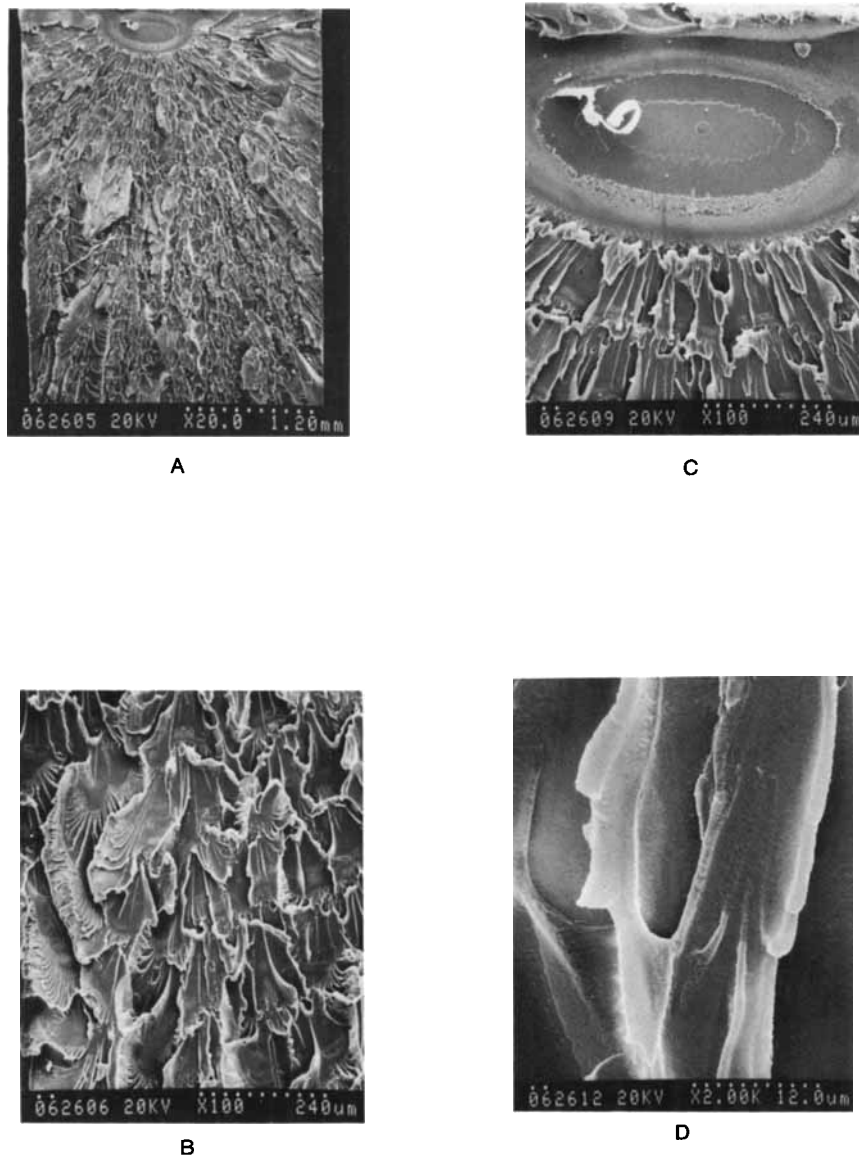
Figure 7   SEM micrographs of the semi-ductile fracture surface, (A) original magnification ×20, front portion; (B) original magnification ×100, middle section; (C) original magnification ×100, plane strain zone close to notch tip; (D) original magnification ×20000, middle section.

strain, the crack proceeding through this region will exceed local shear yielding stress relatively easily with resulting extensive localized shear yielding, as shown by the SEM micrographs [Fig. 7(B)]. The brittle mode has relatively smaller strain at the onset of crack initiation and the portion that will reach shear yielding stress during fracture is considerably less; the majority concentrate near the crack tip in the front part. This proposed mechanism also offers a reasonable interpretation of why the front part of the brittle fracture surface is rough but rear portion is flat and mirror-like. Fraser et al.[16] reported that

razor-notched (the smallest notch radius obtainable) specimens of polycarbonate had the lowest toughness and that the mirror zone covers the whole specimen. This is due to extremely low strain at the onset of crack initiation which results in very little localized shear yielding even at the start of crack.

Two-Dimensional Fracture Mode Diagram of Polycarbonate

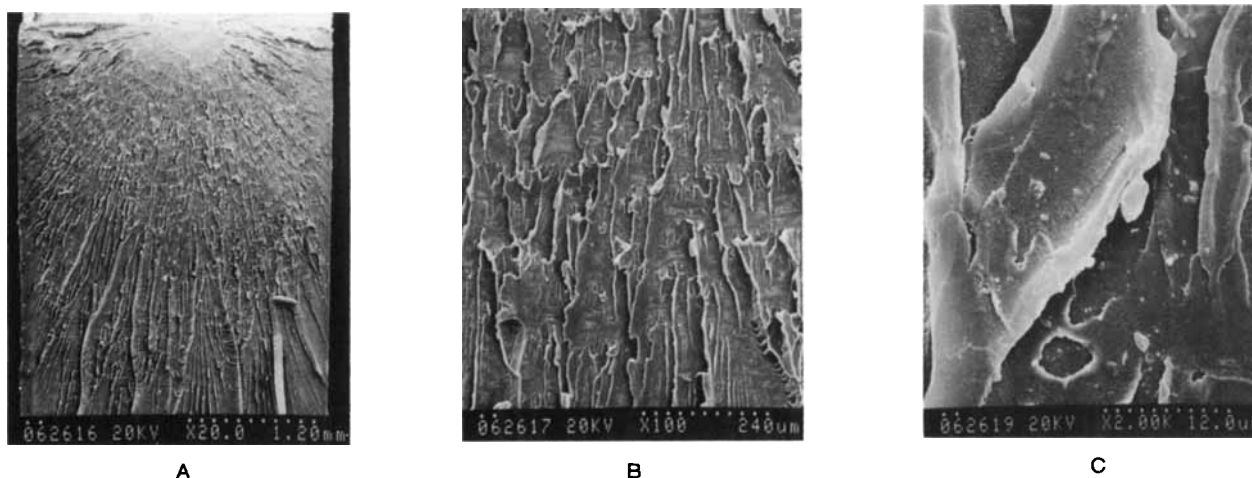Based on our limited available data, a two-dimensional fracture mode diagram in terms of tempera-

A   B   C

Figure 8 SEM micrographs of the brittle fracture surface, (A) original magnification ×20, front portion; (B) original magnification ×100, middle section; (C) original magnification ×2000, middle section.

ture and notch radius has been constructed in Figure 9. Two unstable zones, brittle versus semi-ductile and ductile versus brittle are shown as shaded areas. Three modes coexisting under one set of testing conditions can be expected anywhere between line A–B. If the testing conditions are located closer to point A, a higher probability of semi-brittle than brittle fracture is anticipated. Table I shows 25% of specimens fracture in the ductile mode, 50% in the brittle mode and 25% in the semi-ductile mode. This indicates that the experimental point C is located closer to point A than point B. For the unstable zone, ductile versus brittle, there are not enough data points to give the exact boundary of this zone. If we

take another type of semi-ductile mode such as the one observed by Fraser[16] into consideration, and couple this with the ductile versus brittle unstable zone, there must exist theoretically at least several additional transition zones clustered somewhere around this ductile versus brittle unstable zone. This diagram is based on variables of temperature and notch radius, and significant changes can be expected if the impact rate or specimen thickness (or any other variable) is changed. This plotted mode diagram gives a reasonable explanation for the co-existence of triplet modes and even predicts other conditions may also exist for the triplet modes.

Table I   Izod Impact Strength Around Critical Transition Temperatures (ft lb/in)[a]

Temp. °C	Ductile	Semi-Ductile	Brittle
−30	12.7, 12.4, 12.5, 12.3, 12.0, 12.1, 12.2, 11.9, 12.5, 12.1 (Ave. = 12.3)	None	None
−40	12.3, 12.3, 12.1, 12.9, 12.2 (Ave. = 12.36)	8.73, 8.14, 6.50, 8.20, 7.14, 7.61, 8.78, 8.90, 8.90, 9.19, 8.20 (Ave. = 8.17)	2.28, 1.23, 2.23, 1.29 (Ave. = 1.76)
−50	None	5.80, 6.94, 8.31, 8.84, 8.20, 9.22, 6.68 (Ave. = 7.71)	1.82, 2.05, 1.93 (Ave. = 1.93)
−60	None	4.16, 4.28 4.09, 4.40, 4.25 (Ave. = 4.23)	2.05, 1.99, 2.15, 1.89, 1.90 (Ave. = 1.99)

[a] Polycarbonate, MFR = 15, ⅛-inch thickness, notch radius 21 mil.

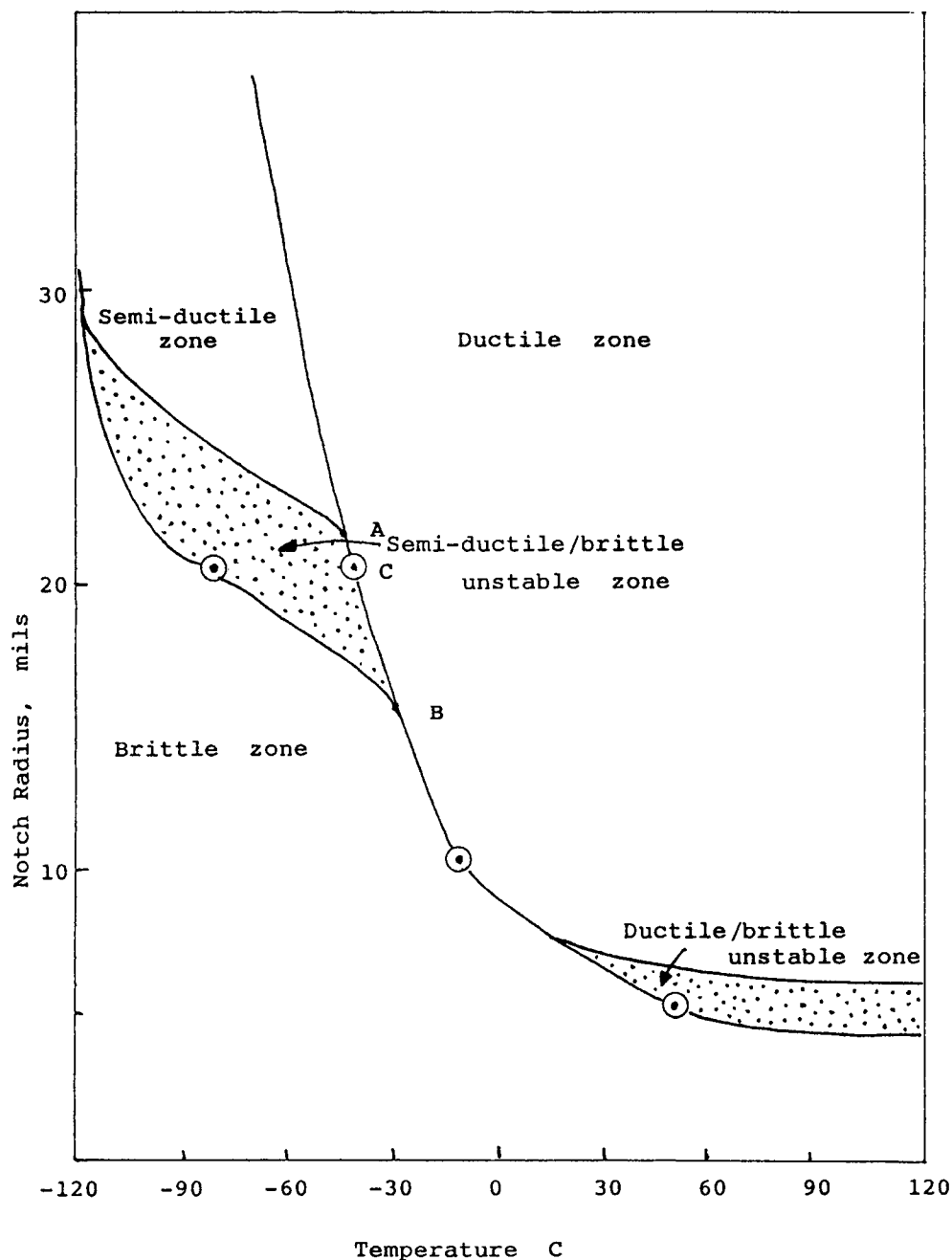**Figure 9** Two-dimensional fracture mode diagram in terms of notch radius and temperature.

REFERENCES

1. G. L. Pitman, I. M. Ward, and R. A. Duckett, *J. Mater. Sci.*, **13**, 2092 (1978).
2. H. R. Brown, *J. Mater. Sci.*, **17**, 469 (1982).
3. D. Hull and T. W. Owen, *J. Polym. Sci., Polym. Phys. Ed.*, **11**, 2039 (1973).
4. F. C. Chang and L. H. Chu, *J. Appl. Polym. Sci.*, to appear.
5. F. C. Chang and H. C. Hsu, *J. Appl. Polym. Sci.*, to appear.
6. C. K. Riew and R. W. Smith, *Rubber-Toughened Plastics*. C. K. Riew, Ed., Advances in Chemistry, No. 222, Am. Chem. Soc., Washington, DC, 1989, p. 225.

7. J. T. Ryan, *Polym. Eng. Sci.*, **18**, 264 (1978).
8. F. C. Chang and L. H. Chu, *Polymer Materials: Sci. Eng.*, **60**, 851 (1989).
9. J. Heijboer, *J. Polym. Sci., C*, **16**, 3755 (1968).
10. G. Allen, D. C. W. Morley, and T. Williams, *J. Mater. Sci.*, **8**, 1449 (1973).
11. R. Ravetti, W. W. Gerberich, and T. E. Hutchinson, *J. Mater. Sci.*, **10**, 1441 (1975).
12. M. Parvin, J. G. Williams, *J. Mater. Sci.*, **10**, 1883 (1975).
13. S. Havriliak, Jr. and V. E. Malpass, ANTEC'85, 645 (1985).
14. L. E. Hornberger, G. Fan, and K. L. DeVries, *J. Appl. Phys.*, **60**, 2678 (1986).
15. H. C. Hsu and F. C. Chang, *Proc. of the 13th ROC Polym. Symp.*, Hsinchu, Taiwan, p. 796 (1990).
16. R. A. W. Fraser and I. M. Ward, *J. Mater. Sci.*, **12**, 459 (1977).
17. A. F. Yee, *J. Mater. Sci.*, **12**, 757 (1977).
18. M. E. J. Dekkers and S. Y. Hobbs, *Polym. Eng. Sci.*, **27**, 1164 (1987).
19. H. C. Hsu and F. C. Chang, *Proc. of the 1990 Annual. Conf. of the Chinese Soc. for Mater. Sci.*, Hsinchu, Taiwan, p. 1005 (1990).
20. C. E. Inglis, *Trans. Inst. Naval Archit.*, **55**, 219 (1913).
21. A. A. Griffith, *Phil. Trans. Royal Soc.*, **A211**, 163 (1921).
22. A. J. Kinloch and J. G. Williams, *J. Mater. Sci.*, **15**, 987 (1980).
23. S. Yamini and R. J. Young, *J. Mater. Sci.*, **15**, 1823 (1980).
24. F. J. Furno, R. S. Webb, and N. P. Cook, *J. Appl. Polym. Sci.*, **8**, 101 (1964).
25. C. Bauwens-Crowet, J. C. Bauwens, and G. Homes, *J. Polym. Sci., A2*, **7**, 735 (1969).
26. H. Eyring, *J. Chem. Phys.*, **4**, 283 (1936).
27. T. Ree and H. Eyring, in *Rheology*, F. R. Eirich, Ed., Vol. 2, Academic Press, New York, 1958, p. 83.